AGU PUBLICATIONS

Geophysical Research Letters

RESEARCH LETTER
10.1002/2017GL073773

Key Points:
- Lake area, level, and volume vary in three stages: slight decrease (1970s–1995), rapid increase (1996–2010), and recent slowdown (2011–2015)
- Lake and groundwater storage both increased at similar rates in Tibetan Plateau's endorheic basin over 2003–2009
- Increased precipitation contributes a major water supply (74%) for lake volume increase, followed by glacier melting (13%) in 2003–2009

Supporting Information:
- Supporting Information S1

Correspondence to:
G. Zhang,
guoqing.zhang@itpcas.ac.cn

Citation:
Zhang, G., et al. (2017), Lake volume and groundwater storage variations in Tibetan Plateau's endorheic basin, *Geophys. Res. Lett.*, *44*, 5550–5560, doi:10.1002/2017GL073773.

Received 13 MAR 2017
Accepted 27 APR 2017
Accepted article online 2 MAY 2017
Published online 2 JUN 2017

Lake volume and groundwater storage variations in Tibetan Plateau's endorheic basin

Guoqing Zhang[1,2], Tandong Yao[1,2], C. K. Shum[3,4], Shuang Yi[5], Kun Yang[1,2], Hongjie Xie[6], Wei Feng[4], Tobias Bolch[7,8], Lei Wang[1,2], Ali Behrangi[9], Hongbo Zhang[1], Weicai Wang[1,2], Yang Xiang[1], and Jinyuan Yu[1,10]

[1]Key Laboratory of Tibetan Environmental Changes and Land Surface Processes, Institute of Tibetan Plateau Research, Chinese Academy of Sciences, Beijing, China, [2]CAS Center for Excellence in Tibetan Plateau Earth Sciences, Beijing, China, [3]Division of Geodetic Science, School of Earth Sciences, Ohio State University, Columbus, Ohio, USA, [4]State Key Laboratory of Geodesy and Earth's Dynamics, Institute of Geodesy and Geophysics, CAS, Wuhan, Hubei, China, [5]Department of Natural History Sciences, Hokkaido University, Sapporo, Japan, [6]Laboratory for Remote Sensing and Geoinformatics, University of Texas at San Antonio, San Antonio, Texas, USA, [7]Department of Geography, University of Zurich, Zürich, Switzerland, [8]Institute for Cartography, Technische Universität Dresden, Dresden, Germany, [9]Jet Propulsion Laboratory, California Institute of Technology, Pasadena, California, USA, [10]Department of Resource Exploration and Civil Engineering, College of Engineering, Tibet University, Lhasa, Xizang, China

Abstract The Tibetan Plateau (TP), the highest and largest plateau in the world, with complex and competing cryospheric-hydrologic-geodynamic processes, is particularly sensitive to anthropogenic warming. The quantitative water mass budget in the TP is poorly known. Here we examine annual changes in lake area, level, and volume during 1970s–2015. We find that a complex pattern of lake volume changes during 1970s–2015: a slight decrease of -2.78 Gt yr^{-1} during 1970s–1995, followed by a rapid increase of 12.53 Gt yr^{-1} during 1996–2010, and then a recent deceleration (1.46 Gt yr^{-1}) during 2011–2015. We then estimated the recent water mass budget for the Inner TP, 2003–2009, including changes in terrestrial water storage, lake volume, glacier mass, snow water equivalent (SWE), soil moisture, and permafrost. The dominant components of water mass budget, namely, changes in lake volume (7.72 ± 0.63 Gt yr^{-1}) and groundwater storage (5.01 ± 1.59 Gt yr^{-1}), increased at similar rates. We find that increased net precipitation contributes the majority of water supply (74%) for the lake volume increase, followed by glacier mass loss (13%), and ground ice melt due to permafrost degradation (12%). Other term such as SWE (1%) makes a relatively small contribution. These results suggest that the hydrologic cycle in the TP has intensified remarkably during recent decades.

1. Introduction

The Tibetan Plateau (TP) has an average elevation of greater than 4000 m with an extensive distribution of glaciers, permafrost, and alpine lakes [*Li et al.*, 2008; *Yao et al.*, 2012; *Zhang et al.*, 2014]. The TP together with its surrounding regions is often referred to as "the Third Pole of the Earth" [*Qiu*, 2008] and the "roof and the world." Lakes, snow, glaciers, and river are important components of the hydrologic cycle in the large high-elevation region. Lakes in the endorheic (closed) basin of the Inner TP have a special role because they form a node linking atmospheric, cryospheric, and biospheric components of the hydrological cycle. Lakes are sensitive to climate change, responding rapidly to environmental changes in their catchments [*Adrian et al.*, 2009]. Because there are few disturbances from human activities in the Inner TP, these lakes provide a unique indicator of climate change.

In the past few decades, lake area in the TP has been undergoing an obvious increase; this is the opposite of changes in other regions of China [*Ma et al.*, 2010], Asia's plateaus [*Zhang et al.*, 2017a], and other regions or drainage basins across the globe [*Donchyts et al.*, 2016; *Pekel et al.*, 2016]. Lake area changes in the TP has been examined using Landsat data with relatively long time spans (a decade or longer) [*Ma et al.*, 2010; *Song et al.*, 2013; *Wan et al.*, 2016; *Zhang et al.*, 2014]. A global water-body mapping at annual scale between 1984 and 2015 is available [*Pekel et al.*, 2016], but manual identification and removal of rivers, reservoirs, and wetland polygons are necessary [*Messager et al.*, 2016; *Zhang et al.*, 2017b]. Lake level change can be retrieved from laser or radar altimetry [*Crétaux et al.*, 2011; *Kleinherenbrink et al.*, 2015; *Zhang et al.*, 2011b]. Combining water level change with lake area can then give estimates

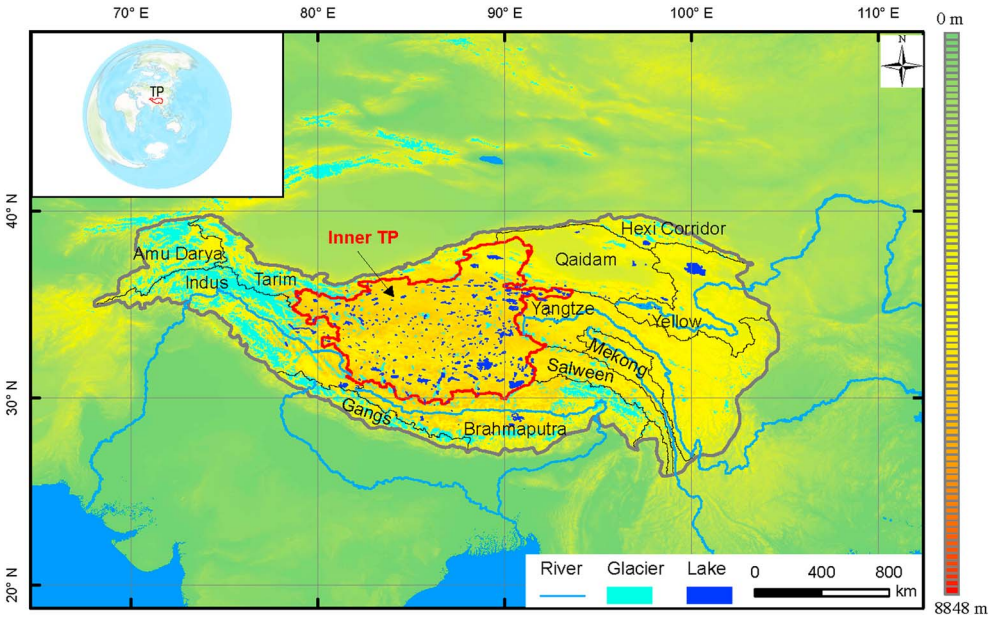

Figure 1. Distribution of lakes, glaciers, and rivers in the Tibetan Plateau (TP). The TP is divided into 12 river basins. The lakes are predominately located in the Inner TP, an endorheic basin (the red polygon). Inset shows the location of TP in the world.

of variations in lake water volume [*Song et al.*, 2013; *Yang et al.*, 2017; *Zhang et al.*, 2013a, 2013b]. For example, water volume changes of 11 large lakes in the southern TP between 1992 and 2015 have been estimated [*Crétaux et al.*, 2016].

A quantitative evaluation of the water balance of each lake on the TP is currently not feasible because of the scarcity of in situ observations. Only a few lakes have had their water budgets quantitatively assessed, namely: Selin Co, Nam Co, Tangra Yumco, Mapam Yumco, and Paiku Co [*Biskop et al.*, 2015; *Li et al.*, 2017; *Tong et al.*, 2016; *Zhou et al.*, 2015, 2013; *Zhu et al.*, 2010] (Table S1 in the supporting information). However, there are more than 1200 lakes (>1 km^2) in the TP, mainly in the Inner TP [*Zhang et al.*, 2014], and 5000 small glacial lakes in the Himalayas [*Zhang et al.*, 2015]. Thus, our knowledge of lake water balance is very limited. In addition, the mass balance in the Inner TP has shown an increase [*Neckel et al.*, 2014; *Yi and Sun*, 2014]. However, the quantitative fractions of mass change have not been assessed.

In this study, we examine annual variations in lake area, water level, and volume in the TP from 1970s to 2015. Within the TP there are 12 large basins, but the Inner TP is a large endorheic basin (7.08×10^5 km^2) with the predominant lake number and area in High Mountain Asia (Figure 1). We conduct a quantitative study of water mass balance for this basin.

2. Data and Methods Used

2.1. Lake Area, Level, and Volume

The Landsat series of satellites are the most popular for lake area mapping because of the long period of data availability, relatively high spatial resolution, and open access [*Pekel et al.*, 2016; *Sheng et al.*, 2016; *Verpoorter et al.*, 2014]. In this study, the Landsat data with free or small fraction of cloud coverage in October were used. If no data were available in October, data from September or November were chosen. The data were also used to extend the available lake observations if the average cloud coverage in a scene is high but cloud cover over several lake surfaces is small. The normalized difference water index [*McFeeters*, 1996] with the optimal threshold determined from the Otsu method [*Otsu*, 1979] was applied to distinguish water from non-water features. Visual examination and manual editing of lake boundaries were conducted combining the false color composition (Bands 5, 4, and 3 as red, green, and blue) of raw Landsat images for each lake. Lakes larger than 10 km^2 were selected: these large lakes dominate the total lake area, and the smaller lakes (<10 km^2) are more liable to fluctuate from year to year [*Zhang et al.*, 2014]. Relative lake area change was

used to estimate the trend of area change [*Tao et al.*, 2015]. The annual Landsat MSS record in 1972–1976 is limited, so data from 1972 to 1976 were grouped into a single period from hereafter referred to as "1970s."

Lake level monitoring has been possible using laser and radar satellite data [*Crétaux et al.*, 2011, 2016; *Zhang et al.*, 2011b]. Here we used the ICESat/GLA14 Release-34 elevation data to retrieve the elevation of lake water surfaces on the TP between 2003 and 2009. The inside buffer of lake boundary delineated from Landsat data in the same year as the ICESat data was used to extract ICESat footprints over the water surface. The mean elevation of selected footprints in each track was calculated as the elevation on the track date. Data from other satellite altimetry missions including TOPEX/POSEIDON, Geosat-Followon, ERS-2, Jason-1/-2, and Envisat [*Crétaux et al.*, 2011, 2016] and Cryosat-2 [*Jiang et al.*, 2017; *Kleinherenbrink et al.*, 2015] have the abilities to monitor TP's lakes with longer data spans and with seasonal coverage, as opposed to the use of ICESat. However, we used ICESat data only primarily because of its advantage of 91 day repeat orbit and its small footprints (70 m), which has an advantage to cover many more lakes than radar altimeter data.

Figure S1 in the supporting information shows the time series of water level for Qinghai Lake from ICESat, station observation, and lake area from Landsat between 1970s and 2015. The patterns of lake level reconstructed using hypsometric (area-altitude) analysis and in situ measurement match well. Finally, we reproduce lake level during 1970s–2015 for lakes with available data (Table S2). Lake water volume change can be estimated using the following equation:

$$\Delta V = (H_{\text{start}} - H_{\text{end}}) \times \left(A_{\text{start}} + A_{\text{end}} + \sqrt{A_{\text{start}} \times A_{\text{end}}}\right)/3 \quad (1)$$

where ΔV is the volume variation and H_{start}, A_{start} and H_{end}, A_{end} are the elevation and area in the start year and end year, respectively. A comparison of water volume change for Nam Co between hypsometric analysis and bathymetry measurement [*Zhang et al.*, 2011a] shows high accuracy (R^2 = 0.98) (Figure S2). The lake volume in 1970s is used as the base year. The relative volume change after 1970s is calculated using equation (1). Total lake water volumes in 2003, 2009, and other years with available data (for lakes >1 km^2) relative to 1970s were also estimated.

2.2. Water Mass Budget

The change in terrestrial water storage (TWS) in the TP includes lake water (L), glacier (G), snow water equivalent (SWE), soil moisture (SM), ground ice stored in permafrost (PM), and groundwater storage (GWS). To quantify the fraction from TWS changes, at least six of the seven components need to be known. The mass budget is expressed as

$$\Delta\text{TWS} = \Delta L + \Delta G + \Delta\text{SWE} + \Delta\text{SM} + \Delta\text{PM} + \Delta\text{GWS} \quad (2)$$

Lake volume changes can be estimated by combining lake area and lake level variations. The glacier mass budget can be observed from ICESat data in 2003–2009 [*Gardner et al.*, 2013; *Kääb et al.*, 2015; *Neckel et al.*, 2014].

In addition, water balance for closed (endorheic) lake or lakes in the endorheic basin can be estimated as

$$\Delta L = \Delta G + \Delta\text{SWE} + \Delta\text{PM} + \Delta P \quad (3)$$

where ΔP is the change in net precipitation (precipitation minus evaporation) over the lake surface and precipitation-induced land runoff. The trends of TWS, SWE, and SM changes and their uncertainties are estimated from a least squares fit after annual and semiannual variations have been removed [*Chen et al.*, 2013].

2.2.1. Mass Change From Gravity Recovery and Climate Experiment Observations

Satellite gravity measurements from the Gravity Recovery and Climate Experiment (GRACE) provide quantitative measurements of TWS changes with unprecedented accuracy. A multibasin inversion method [*Yi et al.*, 2016] is adopted to estimate mass change based on GRACE observations. This method fits total mass in each so-called "mascon" (mass concentration, an area that shares a uniform change pattern) instead of gridded observations or spherical harmonics; thus, the number of fitting variables is greatly reduced and the signal-to-noise ratio of each variable is improved. A weighted function based on the area of each basin is also incorporated, and a regularization factor is also applied to reduce singularities in the inversion.

The method requires a priori mascon divisions. There are 44 mascons at a resolution of 0.5° by 0.5°. The Inner TP is separated from the surrounding basins to reduce the boundary effect from peripheral signal sources

(Figure S3). The surrounding basins are generally sized 5° by 5°, except those in the Ganges which are based on the boundary of the basin. The inversion details are demonstrated in Figure S4. The observed trend by GRACE is well fitted by our method, and the residuals are quite small. The estimated mass is shown in Figure S4b, where positive mass anomalies appear in the inner TP and negative mass anomalies can be recognized in the Himalayas and northern India. Inverse masses in surrounding mascons are discarded because they are contaminated by peripheral signals. The glacial isostatic adjustment effect is corrected based on the ICE-6G_C deglaciation history and the VM5a earth model [*Peltier et al.*, 2015]. GRACE gravity data provide an alternative and complementary tool for quantifying GWS changes [*Chen et al.*, 2016].

2.2.2. Soil Moisture

The Global Land Data Assimilation System (GLDAS) provides global, high-resolution, near-real-time land surface states (e.g., soil moisture) and fluxes by integrating satellite- and ground-based observations [*Rodell et al.*, 2004]. GLDAS drives four land surface models: Mosaic, Noah, the Community Land Model, and the Variable Infiltration Capacity (VIC). In addition, a monthly global soil moisture data set is produced with the driving input fields including the Climate Prediction Center's monthly precipitation over land from over 17,000 gauges and temperature from global reanalysis data [*Fan*, 2004]. An intercomparison of soil moisture in the Inner TP from these models reveals that the spatial patterns of soil moisture from three of the five models (Mosaic, Noah, and VIC) have good agreement (Figure S5). As in previous studies [*Feng et al.*, 2013; *Xiang et al.*, 2016; *Yi et al.*, 2016], the soil moisture from these three products (Mosaic, Noah, and VIC) is averaged to reduce the model bias.

2.2.3. Snow Water Equivalent

Passive microwave sensors are the most efficient way to retrieve snow depth or snow water equivalent (SWE); they have the advantages of cloud penetration and high sensitivity to water content in the snowpack [*Saraf*, 1999; *Smith and Bookhagen*, 2016]. The scanning multichannel microwave radiometer (SMMR), Special Sensor Microwave/Imager (SSM/I), Special Sensor Microwave Imager/Sounder (SSMI/S), and Advanced Microwave Scanning Radiometer–Earth Observing System (AMSR-E) have been used for SWE estimation since 1978. A comparison of SWE from AMSR-E with station measurements shows that the AMSR-E SWE is overestimated [*Yang et al.*, 2015]. A snow depth data set derived from SMMR, SSM/I, and SSMI/S with validation of CMA (China Meteorological Administration) station observations and intersensor calibrations has been developed across China from 1978 to 2014 [*Che et al.*, 2008; *Dai et al.*, 2015]. The snow depth from this data set is used and converted into SWE with snow density (approximately 0.15 g cm^{-3}) in the TP [*Dai and Che*, 2010].

2.2.4. Permafrost

Discontinuous permafrost is extensively distributed across the TP, especially the Inner TP [*Gruber*, 2012; *Li et al.*, 2008]. Significant permafrost degradation has already occurred in the TP [*Luo et al.*, 2016; *Wu et al.*, 2014; *Yang et al.*, 2010]. Eighteen ground-temperature monitoring sites and 13 active-layer monitoring sites have been established along the 800 km Qinghai-Tibet railroad running from south to north [*Yang et al.*, 2010], but these few site observations are not sufficient to give a basin-based mass estimation, especially as they are located outside the Inner TP. A regional modeling of active-layer depth (ALD) over the TP has been performed for 1980–2001 [*Oelke and Zhang*, 2007]. The ALD data in the Inner TP were extracted from previous studies [*Erkan et al.*, 2011; *Oelke and Zhang*, 2007]. Part of the meltwater from permafrost degradation may be stored as ground ice in the active layer; the released water is estimated using the model from *Xiang et al.* [2016].

In the present study, the lake volumes inferred by lake area and lake level changes were computed and studied for the past four decades, 1970s–2015. The water mass balance was performed for 2003–2009, which was constrained by the availability of data on glacier mass budgets using ICESat (2003–2009) and GRACE (since late 2002). The glacier mass budget in the Inner TP is from the forthcoming HIMAP report (http://himap.org/) and is based on the ICESat measurements from *Gardner et al.* [2013] and *Neckel et al.* [2014].

3. Results and Discussion

3.1. Lake Area, Level, and Volume Changes

Annual change in lake area (each lake >10 km^2) shows that lake area across the entire TP has a slight decrease between 1970s and 1995 (Figure 2a). After that, lake area presents a continuous increase, but a stable, even slight decrease of lake area is mapped in several recent years. The time series of lake area in the Inner TP is overall consistent with that for the entire TP, but the lakes of the Inner TP expanded more

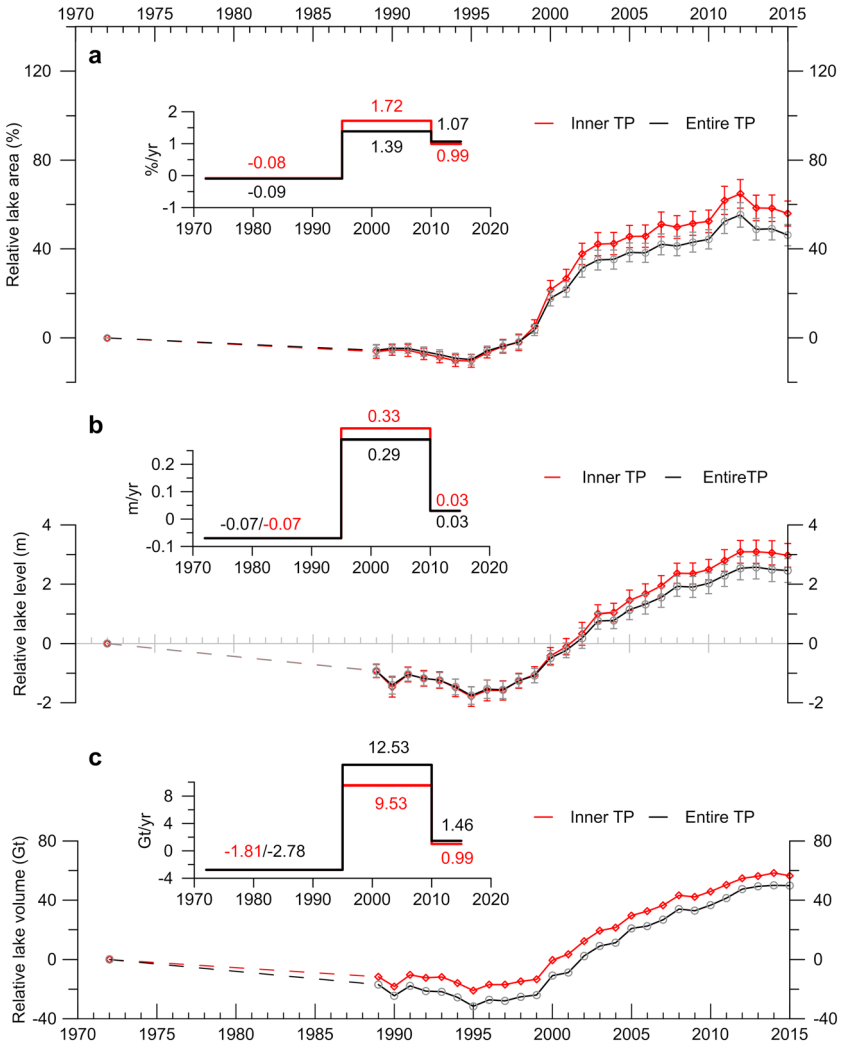

Figure 2. Lake area, level, and water volume changes in the entire TP and the Inner TP between 1970s and 2015. (a) Time series of annual lake area changes relative to 1970s. Inset shows rate of lake area change for all lakes (>1 km^2). (b) Time series of annual lake level changes relative to 1970s. Inset shows rate of lake level change for lakes with available elevation data. (c) Time series of annual water volume changes for lakes with available elevation data relative to 1970s. Inset shows rate of lake volume change for all lakes (>1 km^2).

rapidly than all lakes, and lake area variations in the TP are dominated by those in the Inner TP [*Zhang et al.*, 2017a]. The difference especially appeared after 1998; i.e., the lake area in the Inner TP increased faster than the changes in the entire TP. This could be due to a slight decrease in lake area in the southern TP such as Brahmaputra basin after 1998 [*Zhang et al.*, 2017a]. Figure 3a shows the spatial pattern of lake area change between 1970s and 2015. It is clear that lakes in the northern TP (>31°N) have an increasing rate of expansion. Salt Lake and Selin Co are the two peaks of area change in the histograms. Figure S6 shows that Salt Lake expands rapidly after 2012. Selin Co presents a small area in 1995, but after that the lake's area starts to increase, especially since 1998 (Figure S7). The lakes in the southern TP (<31°N) present a slight shrinkage in area, but the magnitude of the shrinkage is smaller than expansion in the northern TP. In addition, the lake areas in the western TP (<94°E) general expanded in 1970s–2015 but shrank in the eastern TP (>94°E). The total lake area (>1 km^2) had a shrinking rate of −0.09 (−0.08) % per year during 1970s–1995, high expansion rate of 1.39 (1.72) % per year during 1996–2010, and a small increase rate of 1.07 (0.99) % per year in the TP (Inner TP) during 2011–2015, respectively (Figure 2a). The numbers outside and inside the brackets are for the whole TP and for the Inner TP, respectively.

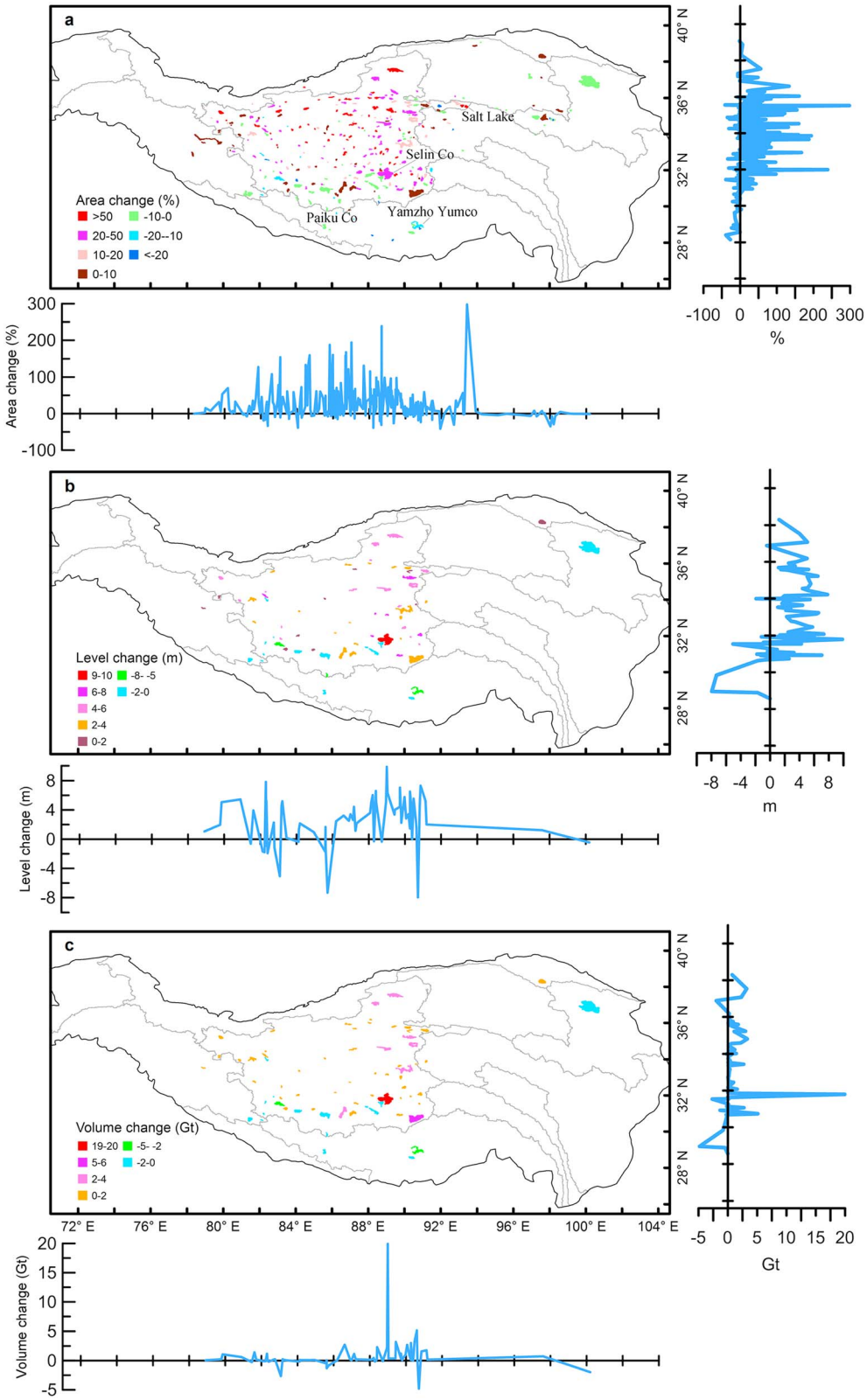

Figure 3. Geographic distribution of lake area, level, and volume change between 1970s and 2015 over the TP. (a) Change (%) in lake area (for lakes with size greater than 10 km^2). (b) Change in lake level (m) (for lakes with available ICESat elevation data). (c) Change in lake water volume (Gt) (for lakes with available ICESat elevation data). Histograms of each subfigure are based on longitude (below) and latitude (right side).

Although many studies have reported lake area changes in the TP [e.g., *Song et al.*, 2013; *Zhang et al.*, 2014, 2017a], this study is the first to provide an annual observation of lake area variations. This high temporal information allows us to examine the evolution of lake stages in a greater detail, which in combination with lake elevation data gives a time series of lake volume change.

Lake level changes derived from ICEsat data in 2003–2009 show an overall increase, especially in the Inner TP (Figure S8). The rate of glacier-fed lake increase (0.24 m yr^{-1}) is slightly higher than that for nonglacier-fed lakes (0.20 m yr^{-1}). For the closed lakes only, the glacier-fed lakes show faster rising water levels (0.26 m yr^{-1}) than nonglacier-fed lakes (0.17 m yr^{-1}). This suggests that the precipitation could be the major driving factor but glacier meltwater provides an additional water supply that results in lake level rising. Based on the hypsometric analysis for the period of 2003–2009, lake levels between 1970s and 2015 were reconstructed. For this it was assumed that during the extrapolated time period, the morphology for each of the lakes is largely regular (J. F. Crétaux, personal communication). However, it cannot be excluded that the morphology of some of the lakes have changed over 40 years. But this has probably a minor impact as high correlation between the lake area and lake level provides some confidence in the assumption (Table S2).

The water level for lakes in the Inner TP increase faster between 1970s and 2015 relative to lakes in the entire TP (Figure 2b). The mean rate of lake level change in the TP (Inner TP) is −0.07 (−0.07) m yr^{-1} during 1970s–1995, 0.29 (0.33) m yr^{-1} during 1996–2010, and 0.03 (0.03) m yr^{-1} during 2011–2015. Selin Co has a remarkable water level increase of 9–10 m, while both Paiku Co and Yamzho Yumco in the southern TP show lake level decrease in the past four decades.

A rate of water storage change in the TP (Inner TP) is −2.78 (−1.81) Gt yr^{-1} during 1970s–1995, 12.53 (9.53) Gt yr^{-1} during 1996–2010, and 1.46 (0.99) Gt yr^{-1} during 2011–2015 (Figure 2c). Selin Co shows a volume increase of 19–20 Gt during 1970s–2015 (Figure 3c). The total lake water volume (>1 km^2) in 1995, 2010, and 2015 relative to 1970s has a change of −69 (−46), 89 (73), and 111 (89) Gt in the TP (Inner TP), respectively (Figure S9).

Overall, lake area, level, and volume changes present three obvious stages: a slight decrease, a continuous increase, and then a tendency to stabilize. The increase of lake area after 1998 accelerates, which could be driven by large-scale atmospheric circulation changes in response to atmospheric warming [*Zhang et al.*, 2017a]. The spatial pattern of lake area, level, and volume change is obvious, with greater increase in the northern TP (dividing at 31°N). Between 1970s and 2015, the mean annual air temperature from CMA stations in the Inner TP (Figure S10) showed a continuous increase (Figure S11). The annual precipitation from both CMA stations and Global Precipitation Climatology Project showed a decrease in 1976–1994, followed by an increase until 2011, and a decrease over the last few years (Figure S11). The precipitation could have played a dominant role in altering the lake change in the Inner TP. However, the limited number of CMA stations in the western TP (Figure S10) prevents the quantitative evaluation of lake water balance. The recent slowdown of lake volume increase is also consistent with the TWS anomaly observed from GRACE data (Figure S11).

3.2. Mass Balance and Lake Water Balance

The mass balance and lake water balance are estimated for the Inner TP based on observation of all the components including TWS, L, G, SWE, SM, and PM. The TWS observed from GRACE data increased at a rate 11.06 ± 1.2 Gt yr^{-1} in 2003–2009 (Figure 4 and Table S3). The lake volume has a significant increase of 7.72 ± 0.63 Gt yr^{-1} over the same period. The small difference of lake volume change between this work and other studies [*Wang et al.*, 2016; *Zhang et al.*, 2013a] could be due to the different total lake areas used. The glaciers experienced a negative mass budget −1.0 ± 0.5 Gt yr^{-1}. Other components such as SWE, SM, and PM are relatively small terms in the mass budget, in comparison to the lake and glacier terms (Table S3). For example, the change in snowpack is 0.04 ± 0.02 Gt yr^{-1}. The GLDAS simulations show an increase (0.21 ± 0.48 Gt yr^{-1}) in surface soil water content in the Inner TP. The permafrost degradation indicates a water release of 0.92 ± 0.46 Gt yr^{-1}. Combining TWS changes and independent estimates of water change in lake, glacier, snow, soil, and permafrost, the groundwater storage is estimated to increase at a rate of 5.01 ± 1.59 Gt yr^{-1}, which is similar to the magnitude of lake water increase.

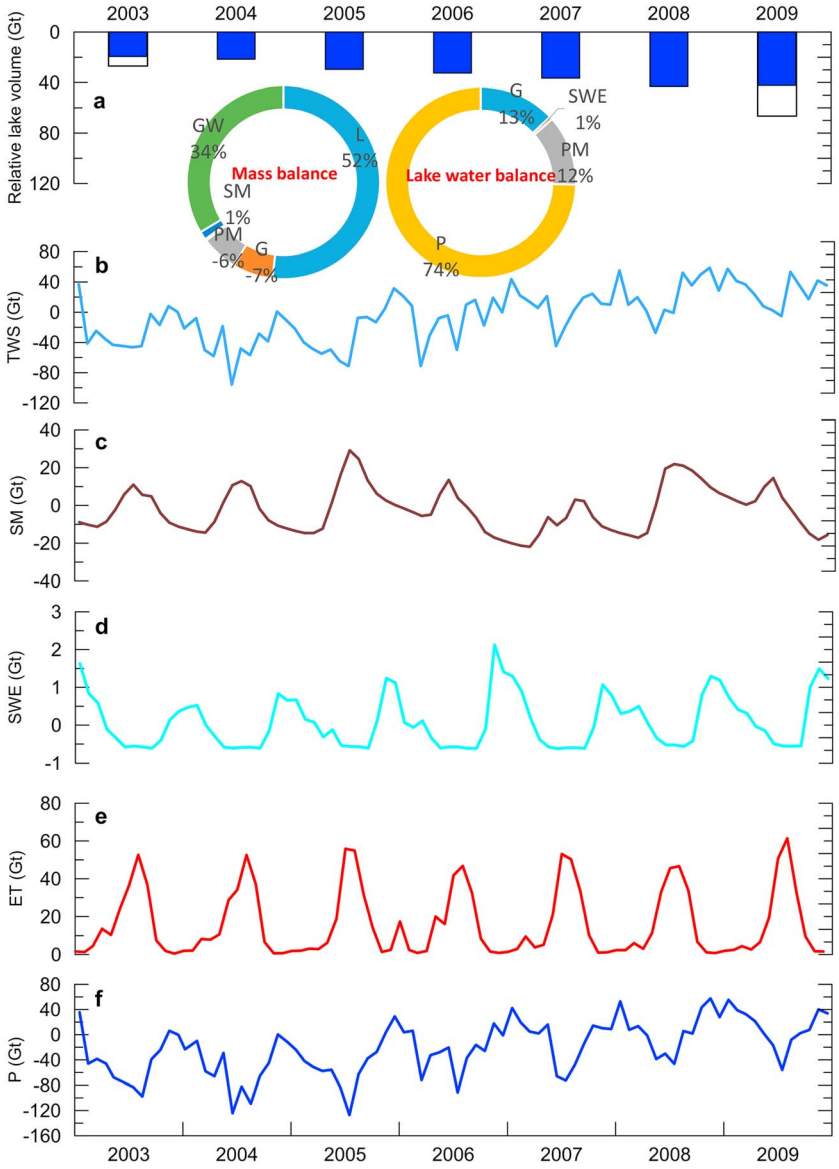

Figure 4. Water balance in the Inner TP between 2003 and 2009. (a) Lake water volume relative to 1970s for lakes with available elevation data. All lake water volumes in 2003 and 2009 are also estimated with gray histogram. Inset shows the ratios of mass balance and lake water balance from lake volume (L), glacier (G), snow water equivalent (SWE), soil moisture (SM), permafrost (PM), groundwater storage (GWS), and net precipitation (P). (b) Terrestrial water storage (TWS) from GRACE observation. (c) SM from averaged GLDAS_NOAH, GLDAS_VIC, and GLDAS_MOSAIC. (d) SWE from SSM/I retrieval. (e) Evapotranspiration (ET). The basin-scale ET in the Inner TP from *Li et al.* [2014]. (f) GRACE-based net precipitation (P) estimation (TWS from GRACE minus evapotranspiration).

From the further lake water balance estimate (Table S3), it is apparent that the increased precipitation is the dominant cause (74%) of lake increase in the TP's endorheic basin during 2003–2009, followed by glacier mass loss (13%) and permafrost degradation (12%). The increase of snowmelt water could be negligible (1%).

These estimates provide the first quantitative evaluation of the mass balance components in the Inner TP. This quantitative water mass balance could been conducted only for the period of 2003–2009, as different satellite data sets are available, e.g., glacier mass budget from ICESat-1 (2003–2009) and mass balance from GRACE-based TWS (after 2003). The analysis of the glacier contribution could potentially be extended back using historical satellite data [e.g., *Bolch et al.*, 2017] or modeling [*Farinotti et al.*, 2015], while TanDEM-X and the forthcoming ICESat-2 provide promising data for the future.

The uncertainty depends on the estimated fraction for each component. The regional glacier mass balance is estimated using ICESat data which provide a reasonable estimate, but glacier coverage is relatively sparse [*Gardner et al.*, 2013; *Neckel et al.*, 2014]. Only fifteen glaciers have in situ measurements of glacier mass balance with only few measurements available before 2000 [*Yao et al.*, 2012]. The station observations of active-layer thickness are limited to those available along the Qinghai-Tibet railroad [*Wu et al.*, 2014]. The long-term snow depth measurements are observed at four CMA stations. The soil moisture network is developed for the central TP around Naqu City from 2010 [*Yang et al.*, 2013]. These ground truth data are limited, considering the large area, complex topography, and variable climate of the high-elevation TP.

A quantitative assessment of lake water balance could be made using a physically based hydrological model. However, the forcing data required would include temperature, precipitation, atmospheric pressure, specific humidity, wind speed, and downward shortwave and longwave radiations. Having long-term measurements from only four CMA stations or short-term observations from automatic weather stations in the Inner TP are a limitation. The remote sensing and reanalysis data sets have shown large uncertainty in retrievals of these parameters [*Behrangi et al.*, 2017; *Tong et al.*, 2014; *Wang and Zeng*, 2012].

The closed basin-scale evapotranspiration (ET) or accumulated precipitation can be estimated by combining the TWS anomaly observation from GRACE temporal gravity measurements [*Behrangi et al.*, 2017; *Li et al.*, 2014]. Based on the TWS anomaly in this study and ET rate of 0.43 ± 0.34 Gt yr^{-1} from *Li et al.* [2014] in the endorheic basin of TP over 2003–2009, the increased precipitation should be 11.49 ± 1.25 Gt yr^{-1}, which is close to the total of increased groundwater storage and lake volume.

The increased change in lake area, level, and water volume has been a quite large contrast to the decreased lake water in other Asian plateaus [*Zhang et al.*, 2017a] and the world's other continents [*Pekel et al.*, 2016]. In addition, the increase of groundwater storage from this study is also comparable to the depletion of groundwater resources in adjacent India [*Asoka et al.*, 2017]. With the development of the meteorological network in the TP, and the maintenance of existing satellite programs and the initiation of new ones, the quantitative understanding of the hydrologic cycle in the TP should continue to improve.

4. Conclusions

The abundant distribution of lakes in the TP, the Third Pole of the Earth, has been regarded as a sensitive indicator and sentinel of climate change. The annual lake area, level, and volume changes in the TP between 1970s and 2015 were examined making maximum use of the available satellite observations. A large increase in water storage has occurred in the endorheic basin (Inner TP or Qiangtang Plateau) of High Mountain Asia compared with other basins within the TP. As a time series, lake change has experienced a slight decrease, a fast increase, and then a recent slowdown. Combining with TWS estimation from GRACE gravity data and other satellite observations, we found that groundwater storage in the Inner TP increased by 5.01 ± 1.59 Gt yr^{-1} over the period of 2003–2009. The groundwater storage change, together with lake water increase, is the major variation in TWS. The increased net precipitation is the dominant factor (74%) for the increase in lake water storage, followed by glacier melting (13%) in 2003–2009. The quantitative water mass balance has been conducted only for the period of 2003–2009, as different satellite data sets are available. TanDEM-X and the forthcoming ICESat-2 are promising data to study the water balance in the near future. In addition, with more available satellite altimeters such as Jason-3, sentinel-3A and 3B, ICESat-2, Jason-CS, and SWOT, more lakes can be observed and a direct estimation of water storage changes of lakes would become possible.

Acknowledgments
This study was supported by grants from the National Natural Science Foundation of China (41571068, 21661132003, 41431070, and 41374020), from the United States National Aeronautics and Space Administration (NNX13AQ89G), and National Science Foundation (ICER-1342644). A. Behrangi is supported by NASA GRACE and GRACE-FO (NNH15ZDA001N—GRACE) program. Part of the research was carried out at the Jet Propulsion Laboratory, California Institute of Technology, under a contract with the National Aeronautics and Space Administration. Parts of this work was conducted within the framework of the NRSCC and ESA Dragon 4 program (ID 32437). We thank Yingying Chen at ITP, CAS, and Longwei Xiang at IGG, CAS, for their help in preparing this manuscript. We thank the USGS for providing the Landsat data (http://glovis.usgs.gov/), NASA for providing ICESat (http://nsidc.org/data/icesat/) and GLDAS (https://ldas.gsfc.nasa.gov/gldas/), and CSR for providing GRACE (http://www.csr.utexas.edu/grace/) used in this study. We acknowledge constructive comments from Jean-Francois Crétaux (Legos/CNES), an anonymous reviewer, and M. Bayani Cadenas, GRL Editor, which resulted in an improved manuscript.

References

Adrian, R., C. M. O'Reilly, H. Zagarese, S. B. Baines, D. O. Hessen, W. Keller, D. M. Livingstone, R. Sommaruga, D. Straile, and E. Van Donk (2009), Lakes as sentinels of climate change, *Limnol. Oceanogr.*, *54*(6), 2283–2297, doi:10.4319/lo.2009.54.6_part_2.2283.

Asoka, A., T. Gleeson, Y. Wada, and V. Mishra (2017), Relative contribution of monsoon precipitation and pumping to changes in groundwater storage in India, *Nat. Geosci.*, doi:10.1038/ngeo2869.

Behrangi, A., A. S. Gardner, J. T. Reager, and J. B. Fisher (2017), Using GRACE to constrain precipitation amount over cold mountainous basins, *Geophys. Res. Lett.*, *44*, 219–227, doi:10.1002/2016GL071832.

Biskop, S., F. Maussion, P. Krause, and M. Fink (2015), What are the key drivers of regional differences in the water balance on the Tibetan Plateau?, *Hydrol. Earth Syst. Sci.*, *20*(1), 209–225, doi:10.5194/hess-20-209-2016.

Bolch, T., T. Pieczonka, K. Mukherjee, and J. Shea (2017), Brief communication: Glaciers in the Hunza catchment (Karakoram) have been nearly in balance since the 1970s, *Cryosphere*, *11*, 531–539, doi:10.5194/tc-11-531-2017.

Che, T., L. Xin, R. Jin, R. Armstrong, and T. Zhang (2008), Snow depth derived from passive microwave remote-sensing data in China, *Ann. Glaciol.*, *49*(1), 145–154, doi:10.3189/172756408787814690.
Chen, J., J. S. Famigliett, B. R. Scanlon, and M. Rodell (2016), Groundwater storage changes: Present status from GRACE observations, *Surv. Geophys.*, *37*(2), 397–417, doi:10.1007/s10712-015-9332-4.
Chen, J. L., C. R. Wilson, and B. D. Tapley (2013), Contribution of ice sheet and mountain glacier melt to recent sea level rise, *Nat. Geosci.*, *6*(7), 549–552, doi:10.1038/ngeo1829.
Crétaux, J. F., et al. (2011), SOLS: A lake database to monitor in the near real time water level and storage variations from remote sensing data, *Adv. Space Res.*, *47*(9), 1497–1507, doi:10.1016/j.asr.2011.01.004.
Crétaux, J. F., R. Abarca-del-Río, M. Bergé-Nguyen, A. Arsen, V. Drolon, G. Clos, and P. Maisongrande (2016), Lake volume monitoring from space, *Surv. Geophys.*, *37*(2), 269–305, doi:10.1007/s10712-016-9362-6.
Dai, L., and T. Che (2010), The spatio-temporal distribution of snow density and its influence factors from 1999 to 2008 in China, *J. Glaciol. Geocryol.*, *32*(5), 861–866.
Dai, L., T. Che, and Y. Ding (2015), Inter-calibrating SMMR, SSM/I and SSMI/S data to improve the consistency of snow-depth products in China, *Remote Sens.*, *7*(6), 7212–7230, doi:10.3390/rs70607212.
Donchyts, G., F. Baart, H. Winsemius, N. Gorelick, J. Kwadijk, and N. van de Giesen (2016), Earth's surface water change over the past 30 years, *Nat. Clim. Change*, *6*(9), 810–813, doi:10.1038/nclimate3111.
Erkan, K., C. K. Shum, L. Wang, J. Guo, C. Jekeli, H. Lee, W. R. Panero, J. Duan, Z. Huang, and H. Wang (2011), Geodetic constraints on the Qinghai-Tibetan Plateau present-day geophysical processes, *Terr. Atmos. Ocean. Sci.*, *22*(2), 241, doi:10.3319/TAO.2010.09.27.01 (TibXS).
Fan, Y. (2004), Climate Prediction Center global monthly soil moisture data set at 0.5° resolution for 1948 to present, *J. Geophys. Res.*, *109*, D10102, doi:10.1029/2003JD004345.
Farinotti, D., L. Longuevergne, G. Moholdt, D. Duethmann, T. Molg, T. Bolch, S. Vorogushyn, and A. Guntner (2015), Substantial glacier mass loss in the Tien Shan over the past 50 years, *Nat. Geosci.*, *8*, 716–722, doi:10.1038/ngeo2513.
Feng, W., M. Zhong, J.-M. Lemoine, R. Biancale, H.-T. Hsu, and J. Xia (2013), Evaluation of groundwater depletion in North China using the Gravity Recovery and Climate Experiment (GRACE) data and ground-based measurements, *Water Resour. Res.*, *49*, 2110–2118, doi:10.1002/wrcr.20192.
Gardner, A. S., et al. (2013), A reconciled estimate of glacier contributions to sea level rise: 2003 to 2009, *Science*, *340*(6134), 852–857, doi:10.1126/science.1234532.
Gruber, S. (2012), Derivation and analysis of a high-resolution estimate of global permafrost zonation, *Cryosphere*, *6*, 221–233, doi:10.5194/tc-6-221-2012.
Jiang, L., K. Nielsen, O. B. Andersen, and P. Bauer-Gottwein (2017), Monitoring recent lake level variations on the Tibetan Plateau using CryoSat-2 SARIn mode data, *J. Hydrol.*, *544*, 109–124, doi:10.1016/j.jhydrol.2016.11.024.
Kääb, A., D. Treichler, C. Nuth, and E. Berthier (2015), Brief communication: Contending estimates of 2003–2008 glacier mass balance over the Pamir–Karakoram–Himalaya, *Cryosphere*, *9*(2), 557–564.
Kleinherenbrink, M., R. C. Lindenbergh, and P. G. Ditmar (2015), Monitoring of lake level changes on the Tibetan Plateau and Tian Shan by retracking Cryosat SARIn waveforms, *J. Hydrol.*, *521*, 119–131, doi:10.1016/j.jhydrol.2014.11.063.
Li, B., J. Zhang, Z. Yu, Z. Liang, L. Chen, and K. Acharya (2017), Climate change driven water budget dynamics of a Tibetan inland lake, *Glob. Planet. Chang.*, *150*, 70–80, doi:10.1016/j.gloplacha.2017.02.003.
Li, X., G. Cheng, H. Jin, E. Kang, T. Che, R. Jin, L. Wu, Z. Nan, J. Wang, and Y. Shen (2008), Cryospheric change in China, *Global Planet. Change*, *62*(3–4), 210–218, doi:10.1016/j.gloplacha.2008.02.001.
Li, X., L. Wang, D. Chen, K. Yang, and A. Wang (2014), Seasonal evapotranspiration changes (1983–2006) of four large basins on the Tibetan Plateau, *J. Geophys. Res. Atmos.*, *119*, 13,079–13,095, doi:10.1002/2014JD022380.
Luo, D., Q. Wu, H. Jin, S. S. Marchenko, L. Lü, and S. Gao (2016), Recent changes in the active layer thickness across the northern hemisphere, *Environ. Earth Sci.*, *75*(7), doi:10.1007/s12665-015-5229-2.
Ma, R., H. Duan, C. Hu, X. Feng, A. Li, W. Ju, J. Jiang, and G. Yang (2010), A half-century of changes in China's lakes: Global warming or human influence?, *Geophys. Res. Lett.*, *37*, L24106, doi:10.1029/2010GL045514.
McFeeters, S. K. (1996), The use of the normalized difference water index (NDWI) in the delineation of open water features, *Int. J. Remote Sens.*, *17*(7), 1425–1432, doi:10.1080/01431169608948714.
Messager, M. L., B. Lehner, G. Grill, I. Nedeva, and O. Schmitt (2016), Estimating the volume and age of water stored in global lakes using a geo-statistical approach, *Nat. Commun.*, *7*, 13603, doi:10.1038/ncomms13603.
Neckel, N., J. Kropáček, T. Bolch, and V. Hochschild (2014), Glacier mass changes on the Tibetan Plateau 2003–2009 derived from ICESat laser altimetry measurements, *Environ. Res. Lett.*, *9*(1), 014009, doi:10.1088/1748-9326/9/1/014009.
Oelke, C., and T. Zhang (2007), Modeling the active-layer depth over the Tibetan Plateau, *Arct. Antarct. Alp. Res.*, *39*(4), 714–722, doi:10.1657/1523-0430(06-200)[oelke]2.0.co;2.
Otsu, N. (1979), A threshold selection method from gray-level histograms, *IEEE Trans. Syst. Man Cybern.*, *9*(1), 62–66, doi:10.1109/TSMC.1979.4310076.
Pekel, J.-F., A. Cottam, N. Gorelick, and A. S. Belward (2016), High-resolution mapping of global surface water and its long-term changes, *Nature*, *540*, 418–422, doi:10.1038/nature20584.
Peltier, W. R., D. F. Argus, and R. Drummond (2015), Space geodesy constrains ICE age terminal deglaciation: The global ICE-6G_C (VM5a) model, *J. Geophys. Res. Solid Earth*, *120*, 450–487, doi:10.1002/2014JB011176.
Qiu, J. (2008), The Third Pole, *Nature*, *454*(7203), 393–396, doi:10.1038/454393a.
Rodell, M., et al. (2004), The Global Land Data Assimilation System, *Bull. Am. Meteorol. Soc.*, *85*(3), 381–394, doi:10.1175/bams-85-3-381.
Saraf, A. K. (1999), Passive microwave data for snow-depth and snow-extent estimations in the Himalayan mountains, *Int. J. Remote Sens.*, *20*(1), 83–95, doi:10.1080/014311699213613.
Sheng, Y., C. Song, J. Wang, E. A. Lyons, B. R. Knox, J. S. Cox, and F. Gao (2016), Representative lake water extent mapping at continental scales using multi-temporal Landsat-8 imagery, *Remote Sens. Environ.*, 129–141, doi:10.1016/j.rse.2015.12.041.
Smith, T., and B. Bookhagen (2016), Assessing uncertainty and sensor biases in passive microwave data across High Mountain Asia, *Remote Sens. Environ.*, *181*, 174–185, doi:10.1016/j.rse.2016.03.037.
Song, C., B. Huang, and L. Ke (2013), Modeling and analysis of lake water storage changes on the Tibetan Plateau using multi-mission satellite data, *Remote Sens. Environ.*, *135*, 25–35, doi:10.1016/j.rse.2013.03.013.
Tao, S., J. Fang, X. Zhao, S. Zhao, H. Shen, H. Hu, Z. Tang, Z. Wang, and Q. Guo (2015), Rapid loss of lakes on the Mongolian Plateau, *Proc. Natl. Acad. Sci. U.S.A.*, *112*(7), 2281–2286, doi:10.1073/pnas.1411748112.

Tong, K., F. Su, D. Yang, L. Zhang, and Z. Hao (2014), Tibetan Plateau precipitation as depicted by gauge observations, reanalyses and satellite retrievals, *Int. J. Climatol.*, *34*(2), 265–285, doi:10.1002/joc.3682.

Tong, K., F. Su, and B. Xu (2016), Quantifying the contribution of glacier-melt water in the expansion of the largest lake in Tibet, *J. Geophys. Res. Atmos.*, *121*, 11,158–11,173, doi:10.1002/2016JD025424.

Verpoorter, C., T. Kutser, D. A. Seekell, and L. J. Tranvik (2014), A global inventory of lakes based on high-resolution satellite imagery, *Geophys. Res. Lett.*, *41*, 6396–6402, doi:10.1002/2014GL060641.

Wan, W., D. Long, Y. Hong, Y. Ma, Y. Yuan, P. Xiao, H. Duan, Z. Han, and X. Gu (2016), A lake data set for the Tibetan Plateau from the 1960s, 2005, and 2014, *Sci. Data*, *3*, 160039, doi:10.1038/sdata.2016.39.

Wang, A., and X. Zeng (2012), Evaluation of multireanalysis products with in situ observations over the Tibetan Plateau, *J. Geophys. Res.*, *117*, D05102, doi:10.1029/2011JD016553.

Wang, Q., S. Yi, and W. Sun (2016), The changing pattern of lake and its contribution to increased mass in the Tibetan Plateau derived from GRACE and ICESat data, *Geophys. J. Int.*, *207*, 528–541, doi:10.1093/gji/ggw293.

Wu, Q., Y. Hou, H. Yun, and Y. Liu (2014), Changes in active-layer thickness and near-surface permafrost between 2002 and 2012 in alpine ecosystems, Qinghai-Xizang (Tibet) Plateau, China, *Global Planet. Change*, *124*, 149–155, doi:10.1016/j.gloplacha.2014.09.002.

Xiang, L., H. Wang, H. Steffen, P. Wu, L. Jia, L. Jiang, and Q. Shen (2016), Groundwater storage changes in the Tibetan Plateau and adjacent areas revealed from GRACE satellite gravity data, *Earth Planet. Sci. Lett.*, *449*, 228–239, doi:10.1016/j.epsl.2016.06.002.

Yang, J., L. Jiang, C. B. Ménard, K. Luojus, J. Lemmetyinen, and J. Pulliainen (2015), Evaluation of snow products over the Tibetan Plateau, *Hydrol. Process.*, 3247–3260, doi:10.1002/hyp.10427.

Yang, K., et al. (2013), A multiscale soil moisture and freeze–thaw monitoring network on the Third Pole, *Bull. Am. Meteorol. Soc.*, *94*(12), 1907–1916, doi:10.1175/BAMS-D-12-00203.1.

Yang, M., F. E. Nelson, N. I. Shiklomanov, D. Guo, and G. Wan (2010), Permafrost degradation and its environmental effects on the Tibetan Plateau: A review of recent research, *Earth Sci. Rev.*, *103*(1–2), 31–44, doi:10.1016/j.earscirev.2010.07.002.

Yang, R., L. Zhu, J. Wang, J. Ju, Q. Ma, F. Turner, and Y. Guo (2017), Spatiotemporal variations in volume of closed lakes on the Tibetan Plateau and their climatic responses from 1976 to 2013, *Clim. Chang.*, *140*(3), 621–633, doi:10.1007/s10584-016-1877-9.

Yao, T., et al. (2012), Different glacier status with atmospheric circulations in Tibetan Plateau and surroundings, *Nat. Clim. Change*, *2*(9), 663–667, doi:10.1038/nclimate1580.

Yi, S., and W. Sun (2014), Evaluation of glacier changes in High Mountain Asia based on 10-year GRACE-RL05 models, *J. Geophys. Res. Solid Earth*, *119*, 2504–2517, doi:10.1002/2013JB010860.

Yi, S., Q. Wang, and W. Sun (2016), Basin mass dynamic changes in China from GRACE based on a multi-basin inversion method, *J. Geophys. Res. Solid Earth*, *121*, 3782–3803, doi:10.1002/2015JB012608.

Zhang, B., Y. Wu, L. Zhu, J. Wang, J. Li, and D. Chen (2011a), Estimation and trend detection of water storage at Nam Co Lake, central Tibetan Plateau, *J. Hydrol.*, *405*(1–2), 161–170, doi:10.1016/j.jhydrol.2011.05.018.

Zhang, G., H. Xie, S. Kang, D. Yi, and S. F. Ackley (2011b), Monitoring lake level changes on the Tibetan Plateau using ICESat altimetry data (2003−2009), *Remote Sens. Environ.*, *115*(7), 1733–1742, doi:10.1016/j.rse.2011.03.005.

Zhang, G., T. Yao, H. Xie, S. Kang, and Y. Lei (2013a), Increased mass over the Tibetan Plateau: From lakes or glaciers?, *Geophys. Res. Lett.*, *40*, 2125–2130, doi:10.1002/grl.50462.

Zhang, G., H. Xie, T. Yao, and S. Kang (2013b), Water balance estimates of ten greatest lakes in China using ICESat and Landsat data, *Chin. Sci. Bull.*, *58*(31), 3815–3829, doi:10.1007/s11434-013-5818-y.

Zhang, G., T. Yao, H. Xie, K. Zhang, and F. Zhu (2014), Lakes' state and abundance across the Tibetan Plateau, *Chin. Sci. Bull.*, *59*(24), 3010–3021, doi:10.1007/s11434-014-0258-x.

Zhang, G., T. Yao, H. Xie, W. Wang, and W. Yang (2015), An inventory of glacial lakes in the Third Pole region and their changes in response to global warming, *Global Planet. Change*, *131*, 148–157, doi:10.1016/j.gloplacha.2015.05.013.

Zhang, G., et al. (2017a), Extensive and drastically different alpine lake changes on Asia's high plateaus during the past four decades, *Geophys. Res. Lett.*, *44*, 252–260, doi:10.1002/2016GL072033.

Zhang, G., J. Li, and G. Zheng (2017b), Lake-area mapping in the Tibetan Plateau: An evaluation of data and methods, *Int. J. Remote Sens.*, *38*(3), 742–772, doi:10.1080/01431161.2016.1271478.

Zhou, J., L. Wang, Y. Zhang, Y. Guo, X. Li, and W. Liu (2015), Exploring the water storage changes in the largest lake (Selin Co) over the Tibetan Plateau during 2003–2012 from a basin-wide hydrological modeling, *Water Resour. Res.*, *51*, 8060–8086, doi:10.1002/2014WR015846.

Zhou, S., S. Kang, F. Chen, and D. R. Joswiak (2013), Water balance observations reveal significant subsurface water seepage from Lake Nam Co, south-central Tibetan Plateau, *J. Hydrol.*, *491*(29), 89–99, doi:10.1016/j.jhydrol.2013.03.030.

Zhu, L. P., M. P. Xie, and Y. H. Wu (2010), Quantitative analysis of lake area variations and the influence factors from 1971 to 2004 in the Nam Co basin of the Tibetan Plateau, *Chin. Sci. Bull.*, *55*(13), 1294–1303, doi:10.1007/s11434-010-0015-8.